

Search for pressure dependence in the sensitivity of several common types of hot-cathode ionization gauges for total pressures down to 10^{-7} Pa

Albert R. Filippelli, and Sharrill Dittmann^{a)}

National Institute of Standards and Technology,^{b)} Gaithersburg, Maryland 20899

(Received 11 February 1991; accepted 20 April 1991)

Dependence of sensitivity on pressure in He, N₂, and H₂ has been investigated for a group of 16 hot-cathode ionization gauges, representing both extractor and Bayard–Alpert types, for total pressure as low as 5×10^{-8} Pa. Absolute sensitivities were determined using a primary high vacuum standard. An independent method, that of measuring the sensitivity ratio of one gauge to another, was also employed. Within a scatter of about $\pm 3\%$, $\pm 4\%$, and $\pm 4\%$ respectively, the N₂, He, and H₂ sensitivity ratio data showed no clearly discernible pressure dependence down to total pressures as small as 5×10^{-8} Pa. The absolute sensitivity measurements in He and N₂ over the range 10^{-7} to 10^{-3} Pa in total pressure, also were constant within a scatter of about $\pm 4\%$ and $\pm 3\%$, respectively. As a consequence of drift in the background component of the total pressure, all the absolute sensitivity measurements at total pressures below 10^{-7} Pa exhibited an apparent pressure dependence not evident in the sensitivity ratio results. In the case of H₂, drift in the pressure persisted at total pressures orders of magnitude larger than the background pressure, and for all the gauges led to an apparent difference of approximately 10% between the H₂ sensitivities at 10^{-8} and 10^{-5} Pa. Results of further investigation suggest that the apparent pressure dependence in the sensitivities is an artifact produced by the well-known phenomenon of thermal dissociation of H₂ at hot filaments and associated processes of H₂ pumping and production of other species such as CO and C₂H₄.

I. INTRODUCTION

The hot-cathode ionization gauge is the most widely and frequently used high vacuum and ultrahigh vacuum (UHV) measuring instrument. In this device, a regulated current of electrons emitted from a hot cathode (filament) is accelerated through a potential difference of typically 100 V maintained in the gauge structure. Some fraction of the flux of energetic electrons will ionize gas phase molecules before the electrons are captured at the accelerating grid. The positive ions are attracted to a collector where most of them are captured, creating a positive collector current. In accordance with simple physical modeling of the gauge, the collector current I_c may be expressed as

$$I_c = I_r + I_e \sum_i S_i P_i, \quad (1)$$

where I_e is the electron emission current, P_i is the partial pressure of gas species i , S_i is the gauge's sensitivity for species i , and I_r is a residual current¹⁻⁴ due to processes other than electron impact ionization of the gas. The pressure value displayed by a commercial ionization gauge controller is proportional to this collector current I_c . Thus, the displayed pressure value depends on the sensitivity values S_i of the particular gauge head in use with the controller.

The sensitivity S_i defined in Eq. (1) is the coefficient which relates ion current developed from gas species i to the gauge's emission current and to the partial pressure of that species. Sensitivity has units of reciprocal pressure and in general, depends on the gauge's geometry and operating parameters (emission current and bias voltages) as well as the gas species and absolute gas temperature. For most UHV hot-cathode ionization gauges under normal operating conditions, the sensitivity also depends on pressure for total

pressures greater than about 10^{-2} Pa, as a result of mean free path and space charge effects.

As the total pressure is decreased below about 10^{-2} Pa, the sensitivities in Eq. (1) are expected to become pressure independent. For He, N₂, and Ar this behavior has been confirmed down to 10^{-6} Pa by a large body of ion gauge calibration data from standards laboratories, including this one.^{5,6} However, for pressures below 10^{-6} Pa there are relatively few published investigations of ion gauge sensitivity.⁷⁻¹² This is due in part to the small number of UHV standards and the difficulty and expense of realizing such standards. Consequently, in almost all cases, pressure measurements with an ionization gauge in the UHV region below 10^{-6} Pa are based on a linear extrapolation of gauge response determined at higher pressures. The possibility of pressure dependence in the sensitivity below 10^{-6} Pa is thus of interest. The present investigation was undertaken with the principal object of examining a group of commonly used ion gauges of both the extractor type (EXG) and the Bayard–Alpert type (BAG) for pressure-dependent sensitivity in the UHV region.

II. APPARATUS

A. Primary high vacuum standard

The 27 cm diam \times 68 cm long stainless steel chamber of the NIST orifice-flow primary high vacuum standard¹³⁻¹⁵ is shown schematically in Fig. 1. A partition separates the chamber into two approximately equal volumes, designated the "upper" chamber and the "lower" chamber. The upper and lower chambers may communicate either through a 13 cm diam hole in this partition or, through a 1.1 cm diam orifice in a movable plate which seals against a liquid gal-

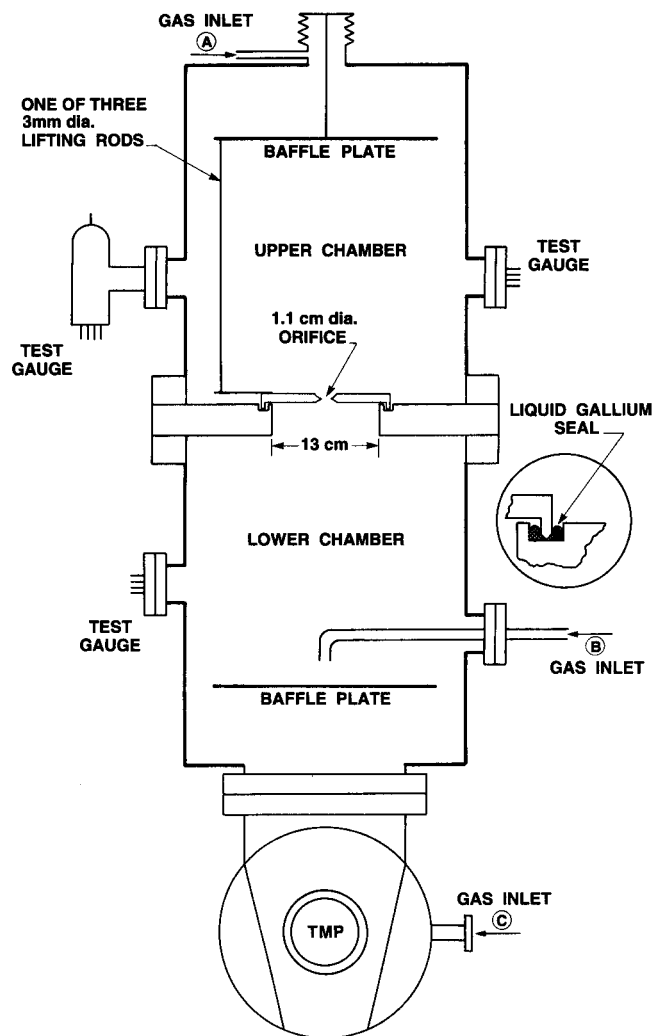


FIG. 1. Schematic diagram of vacuum chamber of the primary standard. The orifice plate is shown in the down position, in which the upper and lower chambers communicate through the 1.1 cm diam orifice.

lium-filled groove in the partition, as shown in Fig. 1. The turbomolecular pump (TMP) has a nominal pumping speed of $0.5 \text{ m}^3 \text{ s}^{-1}$ for N_2 and is backed by a rotary vane pump with a nominal N_2 pumping speed of $0.003 \text{ m}^3 \text{ s}^{-1}$. Relative to the background pressure, the changes in the upper and lower chamber pressures generated with this apparatus are determined by the orifice conductance, the flow of test gas through the system, and the effective TMP speed. These quantities are all calculated or experimentally determined.

As detailed in Ref. 13, this apparatus can be operated as a standard in two configurations. In configuration I, the test gas is introduced into the upper chamber via inlet A, and the movable orifice plate is in its "down" position (as shown in Fig. 1), so that the upper and lower chambers communicate through the 1.1 cm diam orifice. The resulting pressure change ΔP_u in the upper chamber is given in terms of the gas throughput Q and the conductance C of the orifice by

$$\Delta P_u = (Q/C) [R_p / (R_p - 1)], \quad (2)$$

where $R_p \equiv \Delta P_u / \Delta P_l$ is the ratio of the corresponding pressure changes in the upper and lower chambers. The value of the pressure ratio R_p is determined experimentally, using a

throughput sufficiently large ($Q > 4 \times 10^{-5} \text{ Pa m}^3 \text{ s}^{-1}$) that both the upper and lower chamber pressures can be accurately measured with a molecular drag gauge (MDG).^{16,17} For this system R_p has a value of about 27 for N_2 . For configuration I, total systematic error in the generated pressure step in the upper chamber ranges from 1.0% at 10^{-5} Pa to about 1.7% at 10^{-1} Pa . Increasing uncertainty in the measurement of smaller and smaller flows Q sets a practical lower limit of roughly 10^{-7} Pa for the working pressure range in configuration I.

Configuration II extends the useful working range of the apparatus down to about 10^{-8} Pa by allowing a larger, more accurately measurable flow to be used to produce a given size pressure step. Pressures generated in this configuration are usually kept smaller than about 10^{-5} Pa . In this configuration, the test gas is introduced via inlet B into the lower chamber. There is consequently no net flow of gas between the upper and lower chambers, and the pressure changes in the upper and lower chambers will be very nearly equal, independently of whether the orifice plate is in its "up" or "down" position. However, except for the absolute N_2 sensitivity measurements, the orifice plate was in its up position (13 cm diam conductance) in configuration II because it resulted in a lower background pressure in the upper chamber (see Sec. III A). Compared with the pressure change produced by a given flow in configuration I, the pressure change in configuration II is about a factor of C/S smaller, where C is the conductance of the 1.1 cm diam orifice, and S is the effective speed with which the chamber is pumped by the TMP. The exact value of this factor is called the flow ratio R_f where $R_f \equiv Q_u (\Delta P_u) / Q_l (\Delta P_u)$ is the ratio of throughputs into upper chamber (configuration I) and lower chamber (configuration II) required to produce the same pressure change in the upper chamber. Just as for R_p , the value of the flow ratio R_f is experimentally determined. Thus, for configuration II the calculation for the pressure change in the upper chamber becomes¹³

$$\Delta P_u = (Q/C) [R_p / (R_p - 1)] R_f. \quad (3)$$

Ion gauge calibrations at the National Institute of Standards and Technology (NIST) have demonstrated that the technique represented by Eq. (3) consistently produces results which agree within a few tenths of a percent with those obtained with flow into the upper chamber. In configuration II, estimated total systematic uncertainty ranges from 3.7% at 10^{-7} Pa to about 2.5% at 10^{-6} Pa . As discussed in subsequent sections, additional sources of error in the calibrations arise when the gauges themselves change the total pressure and composition of the gas.

In the nonstandard configuration III (not described in Ref. 13) the test gas is introduced through the vent port on the TMP (inlet C of Fig. 1). Thus, the gas reaches the chamber only by backscattering through the pump. Since there is no net flow of gas anywhere in the chamber, this configuration is expected to yield the most uniform pressure distribution. By controlling the flow of gas to inlet C so that the TMP outlet pressure never exceeded about 0.1 Pa, the H_2 pressure in the chamber could be varied from background value to a maximum of about $5 \times 10^{-5} \text{ Pa}$. Similarly

for He, the chamber pressure could be varied from zero up to a maximum of about 2×10^{-5} Pa. N_2 was not used in configuration III because the pump's large compression ratio (10^8) for N_2 limited the maximum N_2 pressure in the chamber to about 10^{-9} Pa.

B. The gauges

Sixteen ionization gauges (see Table I) were studied in this work: one glass-tubulated dual tungsten-filament BAG, eleven nude dual-filament BAGs which fell into six groups with respect to details of materials and construction, three nominally identical EXGs, and one modulated EXG which was however, used without ion current demodulation. In addition, a quadrupole partial pressure analyzer (PPA) was mounted on the upper chamber. All gauges were attached to the chamber (Fig. 1) with metal-gasketed flanges: twelve gauges at locations near the midplane of the upper chamber and four gauges at locations near the midplane of the lower chamber. Absolute sensitivity of the four gauges mounted in the lower chamber could be determined only in configuration II of the system (see Sec. II A above). Elbows and tees were used where necessary to prevent any line-of-sight path between the gauges.

Bias voltages were set at the nominal values indicated by the vendor, and emission currents were set at 1 mA or at the value specified by the vendor. All but two of the gauges were operated with NIST-designed controllers which held bias voltages stable to within ± 0.01 V and emission currents constant to within ± 0.005 mA. Collector currents were measured with an uncertainty of less than 3% using calibrated electrometers. Current measurements on adjacent electrometer ranges agreed to better than $\pm 1\%$.

III. PROCEDURES

A. Bakeout

After the ion gauges were installed, the chamber was evacuated and baked for 8 h at 250°C while being purged with argon gas at about 10^{-4} Pa. The gauges were operated at their normal bias voltages and emission currents during the

bakeout, but no other degassing procedures were used. From extractor gauge measurements and data obtained with the PPA mounted on the upper chamber, the post-bake H_2 partial pressure with all sixteen gauges in operation was estimated to be about 5×10^{-8} Pa and to constitute roughly 90% of the total base pressure when the upper chamber was pumped through the 13 cm diam hole. When pumped through the 1.1 cm diam orifice, the upper chamber base pressure was a factor of 6 to 9 higher.

B. Drift in the background pressure P°

Whenever the conductance between the upper and lower chambers was changed from the 1.1 cm diam orifice to the 13 cm diam hole, or vice versa, the time required for the upper and lower chamber base pressures to reach new steady-state values was much longer than expected, considering the conductances involved and the TMP speed. The time rate of change of the ion gauge collector currents \dot{I}_c was used to judge how close the base pressure was to equilibrium. The very long times required to reach a new equilibrium base pressure are believed to result from pumping and evolution of background gases by the gauges themselves.

Within approximately 3 h after changing from the 13 cm diam conductance to the 1.1 cm diam orifice, the rate of approach of upper chamber gauge collector currents to new equilibrium values had slowed to a value equivalent to a rate of increase of H_2 pressure of about 2×10^{-8} Pa h^{-1} or less. For the sensitivity measurements obtained for $\Delta P > 10^{-6}$ Pa in configuration I, the error introduced by this rate of drift was negligible. On the other hand, for measurements made for $\Delta P < 10^{-7}$ Pa (configuration II), it was eventually found necessary (see discussion of N_2 results in Sec. IV A 2) to wait several days after changing the conductance for the rate of change of base pressure currents to become small enough for reliable sensitivity determinations.

The first measurements made in this work were those in N_2 , and the problem of background pressure drift was not fully appreciated at this time. Examination of the very low pressure N_2 sensitivity results with respect to the time delay

TABLE I. Operating parameters and materials information for the 16 gauges studied in this work.

No. gauges	Type of gauge	Grid material	Filament material	Filament bias (V)	Grid bias (V)	I_e (mA)	Vendor
4	BAG, nude	Pt-Ir	W	45	175	1.00	A
1	BAG, nude	Pt-Ir	W	30	187	1.00	A
1	BAG, nude	...	Th-Ir ^a	30	180	1.00	C
2	BAG, nude	Ta	W	30	180	1.00	B
2	BAG, nude	Mo	W	50	200	1.00	D
1	BAG, nude	W	W	50	150	1.00	E
1	(variable diam grid) BAG	W	W	31	184	1.00	F
3	(glass tubulated) Extractor	Mo	Th-Ir ^a	100	220	1.30	G
1	Modulated Extractor	Mo	Th-Rh ^b	60	240	2.00	J

^a Thoria-coated iridium.

^b Thoria-coated rhenium.

since the change from the 13 cm diam conductance to the 1.1 cm diam orifice, showed a correlation between the length of this time interval and the deviation of the sensitivity measurements from the average sensitivity. Analysis of the effect expected from a base pressure drifting linearly with time shows the difference between the apparent (measured) and a (assumed) constant sensitivity to be proportional to the time delay between the measurement of I_c° and I_c , and inversely proportional to the test gas pressure step.

C. Absolute sensitivity determinations

A gauge's sensitivity S_i to gas species i was determined by measuring the change $\Delta I_c = I_c - I_c^\circ$ in the gauge's collector current I_c resulting from a change in pressure ΔP_i of the test gas, where I_c° is the gauge's collector current before the introduction of any test gas. Assuming that the residual current I_r remains constant, as well as the partial pressures of all gas components except i , Eq. (1) yields

$$\frac{(I_c - I_c^\circ)}{I_c \Delta P_i} = S_i(P_i^\circ + \Delta P_i) + \left(\frac{S_i(P_i^\circ + \Delta P_i) - S_i(P_i^\circ)}{\Delta P_i} \right) P_i^\circ, \quad (4)$$

where $S_i(P_i^\circ + \Delta P_i)$ and $S_i(P_i^\circ)$ are the sensitivity to gas species i at pressure $P_i^\circ + \Delta P_i$ and P_i° , respectively. The absolute sensitivities reported in this work were calculated using the left hand side of Eq. (4), where the test gas pressure change ΔP_i is that determined from the operating parameters of the primary standard, as outlined in Sec. II. A. When $P_i^\circ = 0$ (the case for He and N₂), then the left hand side of Eq. (4) gives the sensitivity S at $P = \Delta P$, even when S has a pressure dependence. However, $P_{H_2}^\circ \neq 0$ because the background is mostly H₂. In this case, pressure dependence in the sensitivity will cause the left hand side of Eq. (4) to differ from the true sensitivity, as defined in Eq. (1), by a small

amount which may be significant only when ΔP is comparable to or smaller than $P_{H_2}^\circ$.

Each data set began with reading the collector currents I_c° at base pressure. Next, a steady flow of test gas was established. When all gauge readings became stable, the flow was measured. During the 20 min required for the flow measurement, the collector current I_c for each gauge was sampled 70–200 times with a computer-controlled electrometer, just as for the I_c° measurements. The data were checked for stability with time and for each gauge an average value of I_c° and I_c was computed from the multiple measurements. Because it would have greatly increased the amount of time and labor to obtain the data, the background signals I_c° were not remeasured between each subsequent test gas pressure increment. In general, the data were always obtained in a sequence of increasing steps in the test gas pressure. This procedure minimized the time delay between measurement of the background I_c° and measurement of the signal change ΔI_c corresponding to the smallest test gas pressure increment.

It should be kept in mind that the absolute sensitivity results will depend upon the behaviour of both the gauges and the primary standard. As mentioned above for example, drifts in the background pressure will cause errors in the value determined for ΔI_c . For this reason, evaluation of the sources of any systematic error in the sensitivity measurements requires data obtained simultaneously for a group of gauges of several types, as well as data obtained by other techniques.

D. Sensitivity ratio determinations

Consider two gauges, gauge a and gauge b , simultaneously exposed to the same pressure step ΔP of a single-component test gas i . From Eq. (1), the ratio R of their corresponding collector current changes is

$$R = \frac{(I_c - I_c^\circ)_a}{(I_c - I_c^\circ)_b} = \frac{(I_c)_a [S_i(\Delta P_i + P_i^\circ)(\Delta P_i + P_i^\circ) - S_i(P_i^\circ)P_i^\circ]_a + E_a}{(I_c)_b [S_i(\Delta P_i + P_i^\circ)(\Delta P_i + P_i^\circ) - S_i(P_i^\circ)P_i^\circ]_b + E_b}, \quad (5)$$

where $S_i(\Delta P_i + P_i^\circ)$ and $S_i(P_i^\circ)$ are the sensitivity to gas species i at pressure $\Delta P_i + P_i^\circ$ and P_i° , respectively. The terms $E_a = [\dot{I}_c^\circ]_a \Delta t$ and $E_b = [\dot{I}_c^\circ]_b \Delta t$ represent the effect of an assumed linear drift in the background level over the time interval Δt between measurement of I_c° and I_c . Since the emission current for each gauge is held constant, determining the value of this ratio serves as a way to investigate pressure dependence in the ratio of their sensitivities, independently of the primary standard. Deviation from constant sensitivity response in either or both of the gauges will be evident as a pressure dependence in the value of R , except in the special case in which both gauges exhibit the same functional dependence of sensitivity on pressure. Because the absolute value of the pressure change is not needed for this method, the data were obtained four to five times more

quickly than was the case for the absolute sensitivity determinations (Sec. III C). Consequently, error in the measurement of $(I_c - I_c^\circ)$ as a result of drift in the background pressure, was greatly reduced because of the much shorter time delay between measurement of I_c and I_c° .

One of the three extractor gauges was arbitrarily selected to serve as gauge b (the reference gauge) in Eq. (5). Gauge a represents each of the other fifteen gauges. For the ratio measurements in He and H₂, the gas was introduced through the vent port on the TMP (inlet C of Fig. 1). In the case of N₂, the gas was introduced via inlet B in the lower chamber. In either case, the upper and lower chamber gauges all simultaneously experienced the same test gas pressure changes, to within a few tenths of a percent. The value of R was computed from the left hand side of Eq. (5), using

only simultaneously measured values of $(\Delta I_c)_a$ and $(\Delta I_c)_b$. Collector current measurements were made only after their values had become time independent or were changing linearly with time over the time interval (about 3 min) of the measurements. Starting with pressure steps as small as 6×10^{-9} Pa, the pressure change ΔP was varied so that the total pressure went from the base vacuum value P° of about 5×10^{-8} Pa ($\Delta P = 0$), to as high as $P^\circ + \Delta P = 10^{-4}$ Pa. For each of the gases, at least two data sets in overlapping pressure ranges were obtained over a period of two days.

IV. RESULTS

A. Nitrogen gas

1. Absolute sensitivities for N_2

Ten independent sets of absolute N_2 sensitivity measurements were made for 14 of the test gauges over a period of two months. Measurements for test gas pressure increments $\Delta P(N_2)$, between 1×10^{-7} Pa and 2×10^{-3} Pa, were used to calculate an arithmetic average sensitivity \bar{S} for each gauge. The values are given in column 5 of Table II. As an indication of repeatability of the absolute sensitivity measurements, note that for each gauge the sample standard deviation about the mean was 1.5% or less. For each gauge the deviations $\Delta S(\%)$, of the individual measurements from the average value for that gauge are plotted in Fig. 2(a) as a function of the N_2 pressure change ΔP . With one exception, discussed below, data for individual gauges are not identified in Fig. 2 because the different gauges did not show different systematic trends with pressure. Figure 2(a) displays results obtained with flow into the lower chamber via inlet B, as well

as results obtained for flow into the upper chamber via inlet A. However, in both cases for these results in N_2 , the upper and lower chambers communicated through the 1.1 cm diam orifice. The deviations plotted in Fig. 2(a) indicate that with one exception, each gauge independently of its type (EXG or BAG) and details of its materials and geometry, has a constant sensitivity response for N_2 to within $\pm 3\%$ for pressure changes as small as 5×10^{-8} Pa.

As shown in Fig. 2(a) for ΔP below 5×10^{-8} Pa, the ΔS results of all the gauges show a systematic increase with decreasing size of the test gas pressure step, as well as a larger scatter in the values. It is believed that this systematic trend is not due to an increase in gauge sensitivity for these very small pressure steps, but rather that it is an artifact produced by a background pressure which was slowly increasing. Changes in collector current caused by a drift in P° cannot be distinguished from those caused by introduction of the test gas. Such drift leads to errors in the calculated sensitivities (see H_2 Sec. IV C 1 below, also). Thus, stability in the background pressure becomes critical to good calibrations whenever ΔP is comparable to or smaller than P° . The vertical reference lines in Fig. 2 indicate values of $\Delta P(N_2)$ which are equivalent to the base vacuum collector current I_c° of upper chamber gauge No. 14: the dashed line corresponds to the case in which the upper and lower chambers communicate through the 1.1 cm diam orifice, and the dotted line corresponds to the 13 cm diam hole. For $\Delta P < 5 \times 10^{-8}$ Pa the increased scatter in the results is attributed to the increasing significance of noise in the measurement of the corresponding current changes ΔI_c .

Although it was not the principal focus of this work, it is

TABLE II. Average N_2 sensitivities, and sensitivities in He and H_2 relative to N_2 , determined for the 16 gauges studied in this work.

Gauge Type	Vendor	Gauge no.	Vendor specified $S [N_2]$ (Pa^{-1})	Measured		
				$\bar{S} [N_2]$ (Pa^{-1})	$\bar{S} [\text{He}]/\bar{S} [N_2]$	$S_0 [H_2]/\bar{S} [N_2]$
Nude	A	1	0.19	0.228	0.157	0.400
BAG	A	3	0.19	0.181	0.154	0.389
	A	5	0.19	0.174	0.164	0.395
	A	7	0.19	0.190	0.165	0.380
	A*	16	0.19	...	0.166	0.372
	B	6	0.19	0.175	0.172	0.374
	B	9	0.19	0.156	0.168	0.373
	C	4	0.075	0.090	0.173	0.363
	D	8	0.19	0.177	0.161	0.375
	D	11	0.19	0.103	0.175	0.407
Nude	E	2	0.038	0.067	0.157	0.444
BAG						
Tub. BAG	F*	15	0.075	...	0.180	0.395
EXG	G	14	0.050	0.064	0.189	0.408
	G	13	0.050	0.059	0.183	0.411
	G	12	0.050	0.065	0.180	0.396
Mod. EXG	J	10	0.056	0.032	0.181	0.350

* Gauge was operated with a commercial controller. Sensitivity ratios were obtained from ratios of experimentally determined calibration factors for the controller display.

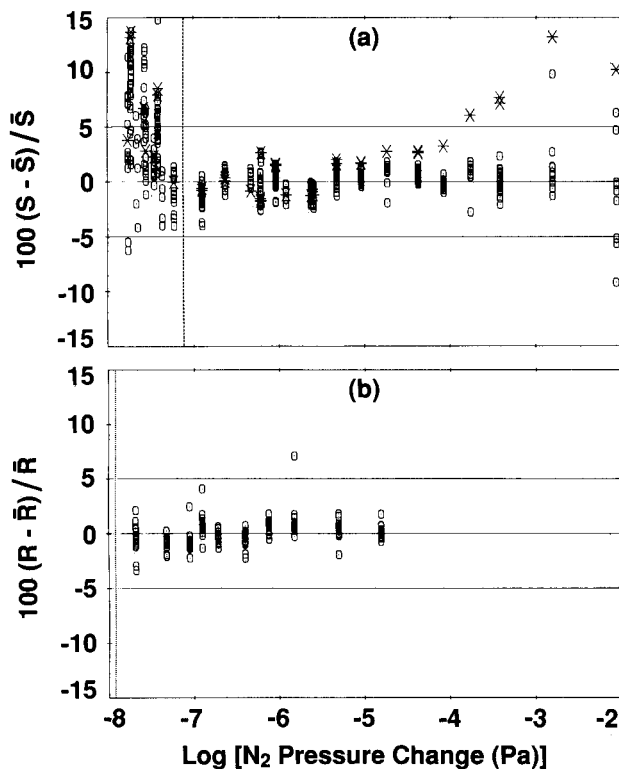


FIG. 2. Sensitivity results in N₂: (a) Deviation of individual absolute sensitivity determinations from average absolute sensitivity \bar{S} [N₂], for each of 14 of the test gauges; (b) Ratio of change in collector current for 15 of the test gauges to the corresponding change in the reference gauge collector current (reference gauge = gauge No. 14), expressed as a % deviation from the average ratio for each gauge. The dashed and dotted vertical reference lines indicate the values of $\Delta P(N_2)$ which are equal to the N₂ pressure equivalent to the base vacuum collector current I_c° of upper chamber gauge No. 14 for the case in which the upper and lower chambers communicate through the 1.1 cm diam orifice or the 13 cm diam hole, respectively.

worth pointing out that at the highest N₂ pressures the response of one of the BAGs [gauge No. 1 in Table II; data identified by * in Fig. 2(a)] became nonlinear above about 10^{-5} Pa. Gauges No. 3, 5, and 7, nominally identical to this one, did not show a nonlinear response in N₂ until the pressure was two orders of magnitude higher. BAG No. 1 also demonstrated a N₂ sensitivity about 25% higher than the other three gauges of the same type. Within a range of about $\pm 4\%$, all four of these gauges showed the same He/N₂ or H₂/N₂ sensitivity ratios (see Table II). While this nonlinearity at higher pressures is expected, it is not usually seen in BAGs in N₂ unless the pressure exceeds about 10^{-3} Pa. The behavior of this gauge illustrates the danger in assuming that a randomly selected gauge of this type will have a linear N₂ response provided that the pressure is below about 10^{-3} Pa. At pressures greater than about 10^{-3} Pa, the onset of this high pressure nonlinearity is evident in the rest of the gauges. The large spread in values at 10^{-2} Pa is not due to increased scatter in the data. It results from the fact that as the pressure is made larger and larger, the onset of nonlinearity in some gauges manifests itself by an increase in sensitivity, while for other gauges the sensitivity simply decreases as the pressure is increased.

2. Sensitivity ratio determinations in N₂

Sensitivity ratios in N₂ were determined for 15 gauges. As pointed out in Sec. III D., the ratio values will be affected much less than the absolute sensitivity results by drift in the background pressure. Even so, the base pressure was allowed to stabilize for more than 24 h before starting these ratio measurements. These ratio data were analyzed in the same manner as the absolute sensitivity data, viz., an arithmetic average value \bar{R} was computed from the individual ratio values as defined in Eq. (5) for each gauge relative to the reference gauge. An extractor gauge (gauge No. 14, Table II) mounted on the upper chamber was used as the reference gauge in this work. Deviations $\Delta R(\%)$ from that average were then computed for each ratio value, where $\Delta R = 100(R - \bar{R})/\bar{R}$. For these ratio measurements, the gas was admitted via inlet B in the lower chamber, and the upper and lower chambers communicated via the 13 cm diam conductance. Individually, the data for the ratio of each gauge's N₂ sensitivity to the N₂ sensitivity of the reference gauge showed no pressure dependence within a scatter of about $\pm 3\%$. For this reason, the data for all the gauges are shown in Fig. 2(b) without identifying the data belonging to any particular gauge. The average absolute N₂ sensitivity for the reference gauge (value in Table II) was used to determine the pressure coordinates for the plot of these ratio data.

Over the interval 5×10^{-8} Pa to 2×10^{-5} Pa the ratio data confirm the pressure independent sensitivity indicated by the results shown in Fig. 2(a). In contrast to the corresponding absolute sensitivity measurements in shown Fig. 2(a), the ratio data shown in Fig. 2(b) also show no pressure dependence below 5×10^{-8} Pa. Since the results obtained by the ratio method are much less influenced by drift in the background pressure P° , the agreement between the two methods strongly suggests that the apparent pressure dependence of absolute sensitivity values at low pressures is an artifact.

B. Helium gas

1. Absolute sensitivities in helium

Seven independent sets of absolute He sensitivity measurements were made for 14 of the gauges over a period of two months. For each upper chamber gauge an average sensitivity \bar{S} was calculated from the data obtained at pressures above 3×10^{-5} Pa; for lower chamber gauges, the average sensitivity was determined from the data obtained below 3×10^{-5} Pa. Column 6 of Table II gives, for each gauge, the ratio of its average He sensitivity to its corresponding average N₂ sensitivity. The deviations $\Delta S(\%)$ of the individual measurements from a gauge's average sensitivity are plotted in Fig. 3(a) as a function of the He pressure change ΔP above the base pressure P° . The vertical reference lines in Fig. 3 indicate the values of $\Delta P(\text{He})$ which are equivalent to the base pressure collector current I_c° of upper chamber gauge No. 14: the dashed line corresponds to the case in which the upper and lower chambers communicate through the 1.1 cm diam orifice, and the dotted line corresponds to the 13 cm diam hole. With regard to these absolute He sensitivity mea-

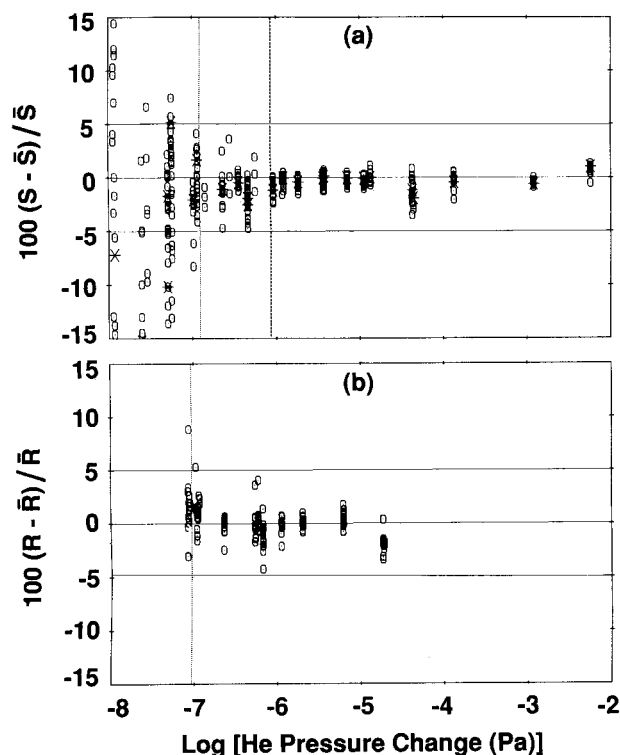


FIG. 3. Sensitivity results in He: (a) Deviation of individual absolute sensitivity determinations from average absolute sensitivity $\bar{S}[\text{He}]$ for each of 14 of the test gauges; (b) Ratio of change in collector current for 15 of the test gauges to the corresponding change in the reference gauge collector current (reference gauge = gauge No. 13), expressed as a % deviation from the average ratio for each gauge. The dashed and dotted vertical reference lines indicate the values of $\Delta P(\text{He})$ which are equal to the He pressure equivalent to base pressure collector current I_c° of upper chamber gauge No. 14, and correspond to the cases in which the upper and lower chambers communicate through the 1.1 cm diam orifice or the 13 cm diam hole, respectively.

surements shown in Fig. 3(a) three things should be noticed.

First, even for the smallest pressure changes ($\Delta P < 10^{-7}$ Pa), there is no indication of a systematic pressure dependence in S . This is not immediately obvious from Fig. 3(a) because data for individual gauges (except one) are not distinguished. However, separate examination of the data for each gauge shows no repeatable pressure dependence in the S values. When the background pressure was slowly increasing ($\dot{I}_c^\circ > 0$) the ΔS values obtained for ΔP below about 10^{-6} Pa tended to be positive and to increase in magnitude as ΔP was made smaller. (This observation is consistent with the same behavior seen in the N_2 data, where $\dot{I}_c^\circ > 0$). Conversely, when the base pressure was decreasing ($\dot{I}_c^\circ < 0$) the ΔS values tended to be negative and again to become larger in magnitude for decreasing size of ΔP . These observations are fully consistent with the effects expected from a drifting base pressure and are believed to be due to nothing more than the effects of a drifting base pressure. The lowest pressure helium results appear to differ from the lowest pressure N_2 results only because Fig. 3(a) includes data for both cases, background increasing and background decreasing.

Second, significant scatter ($> 5\%$) is evident in the He sensitivity results up to a higher pressure (ΔP about 10^{-7}

Pa) than in the N_2 results. This increased scatter in the He results is attributed to the gauges' lower He sensitivity (about $1/6$ that for N_2 —see Table II). For the same size of pressure step ΔP random error in the current measurements will produce a larger scatter for ΔI_c in He than in N_2 .

Third, all the way up to the high end of the investigated pressure range (6×10^{-3} Pa), there is no evidence of nonlinear behavior in any of the gauges, including the one BAG (gauge No. 1 of Table II) which did show a nonlinear response in N_2 above 10^{-5} Pa [data identified by * in both Figs. 2(a) and 3(a)]. The sensitivity data for this particular gauge are as reproducible as any of the other gauges and indicate a pressure independent He sensitivity. (The relatively unusual behavior of this gauge in N_2 may arise from some unrecognized feature of its geometry, although there was nothing obviously unusual about it. This behavior was not studied further, however.)

2. Sensitivity ratio determinations in helium

Sensitivity ratios in He were determined for 15 gauges. The reference gauge was an extractor gauge (gauge No. 13 of Table II) mounted on the upper chamber (not the same EXG as used in the ratio measurements in N_2 , however). The gas was admitted via the TMP vent port (inlet C) and the upper and lower chambers communicated through the 13 cm diam conductance. The data analysis was the same as that applied to the N_2 data. Data for all 15 gauges are shown in Fig. 3(b) without identifying individual gauges, since none of the data exhibited any clear pressure dependence, within a scatter of about $\pm 4\%$. The reference gauge's average absolute He sensitivity (value in Table II) was used to determine the pressure coordinates for the ratio data plotted in Fig. 3(a). Over the interval of these measurements (8×10^{-8} Pa to 2×10^{-5} Pa), these ratio data confirm the constant sensitivity behavior indicated by the corresponding absolute sensitivity measurements shown in Fig. 3(a).

C. Hydrogen gas

1. Absolute sensitivity determinations in H_2

On each of four days during a one week period, an independent set of absolute sensitivity measurements in H_2 was made for 14 of the gauges. The gas was admitted via inlet B and the upper and lower chambers communicated via the 13 cm diam conductance. The results of these four data sets, identified by plotting symbols \times , 0 , $+$, and $*$ are shown in Fig. 4(a). Data for individual gauges are not identified since they all exhibited the same systematic behavior. The dotted vertical reference lines in Fig. 4 indicate the values of $\Delta P(\text{H}_2)$ which are equal to the H_2 pressure equivalent of the base pressure collector current I_c° of upper chamber gauge No. 14.

These sensitivity measurements turned out to be both problematic and instructive. As in the case of N_2 and He, there were uncertainties introduced into the measurements of ΔI_c at very small $\Delta P(\text{H}_2)$ because of drifting base pressure P° (see discussion in Secs. IV A 1 and IV B 1). However, in addition to this, and unlike the case for N_2 and He, whenever the H_2 flow to the chamber was changed from one

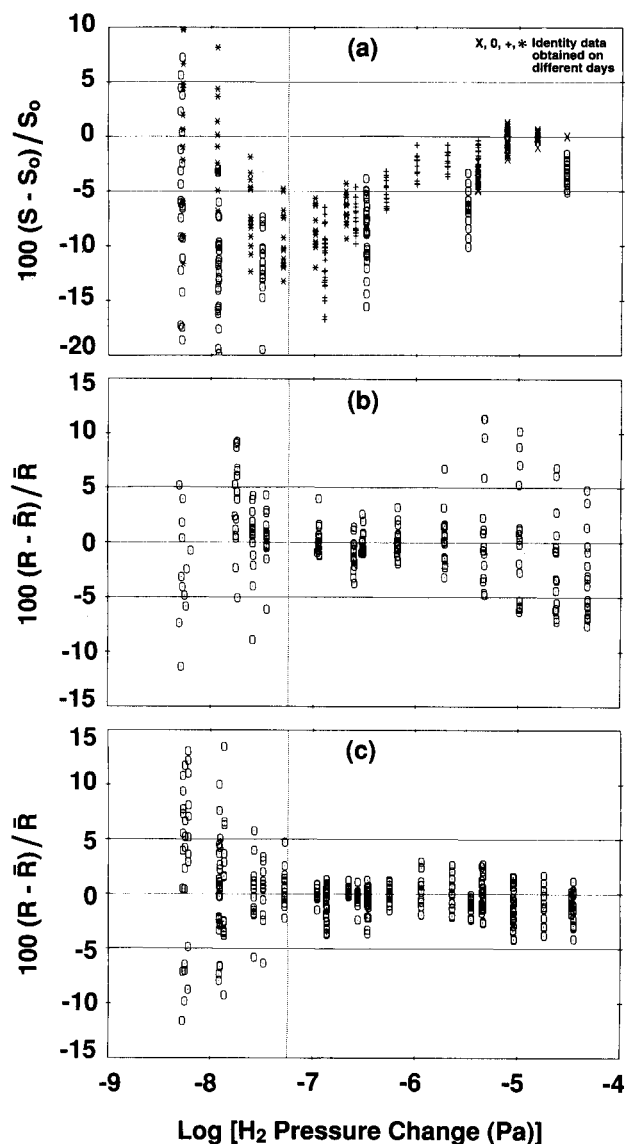


Fig. 4. Sensitivity results in H_2 : (a) Deviation of individual absolute sensitivity determinations for each of 14 of the test gauges from the value $S_0 [H_2]$ determined for that gauge at 3×10^{-5} Pa on day X . Plotting symbols X , 0 , $+$, and $*$ in (a) identify results obtained on each of four days. (b) Ratio of change in collector current to the corresponding change in the reference gauge collector current (reference gauge = gauge No. 14) for 15 of the test gauges, expressed as a % deviation from the average ratio for each gauge; The results shown in (b) were obtained over a two-day period. (c) Alternate analysis of the (a) data, using the method employed in (b). The dotted vertical reference lines indicate the values of $\Delta P(H_2)$ which are equal to the H_2 pressure equivalent to the base pressure collector current I_c of upper chamber gauge No. 14.

constant value to another, the ion gauges' collector currents did *not* promptly assume new values corresponding to the new value of the flow. Instead, the changes ΔI_c asymptotically approached new values. This effect was significant even when the H_2 flow was large enough that $\Delta P(H_2) \gg P^\circ$. At very small flows (corresponding to very small pressure increments $10^{-8} \text{ Pa} \leq \Delta P(H_2) \leq 10^{-7} \text{ Pa}$), the ion gauge collector currents would continue to change for many hours. Faced with this difficulty, the following practice was adopted: the H_2 flow was always changed in a sequence of increasing steps and measurements of ΔI_c were performed after

waiting about 1/2 hour after each change in the flow. It was usually (but not always) found that after 1/2 hour delay, the collector currents were increasing at a rate $\leq 2\%$ per hour. For large flows, corresponding to $\Delta P(H_2) \geq 10^{-5} \text{ Pa}$, the collector currents became time independent and the sensitivity values became pressure independent after approximately 1/2 hour delay. For this reason, the absolute sensitivity results for each gauge are expressed in terms of their deviations $\Delta S(\%)$ from the sensitivity value $S_0 [H_2]$ determined at the *highest* H_2 pressure ($3 \times 10^{-5} \text{ Pa}$ of data set X), rather than as deviations from the average sensitivity. The S_0 values, expressed as a ratio to each gauge's average N_2 sensitivity $\bar{S} [N_2]$ are given in column 7 of Table II.

There is an apparent pressure dependence in these results, with the values at 10^{-5} Pa being about 10% larger than at 10^{-8} Pa . However, as pointed out above, the size of the deviation ($S - S_0$) also depended on the time delay between a change in H_2 flow and measurement of the corresponding change ΔI_c in collector current. This time dependence in the collector currents immediately raised questions: (1) To what extent was it due to a real time dependent sensitivity?¹⁸; (2) To what extent was it caused by a time-dependent pressure as a result of (a) pumping of H_2 by adsorption¹⁹ on the 0.8 m^2 surface area of the vacuum chamber, (b) pumping of H_2 by thermal dissociation of H_2 at the surface of the hot filaments,²⁰⁻²⁴ (c) pumping of H_2 by dissociative electron impact excitation,^{25,26} and (d) production of H_2O , CO , and CO_2 and hydrocarbons (CH_4 , C_2H_4) via reactions of H_2 with C and O in the hot filament material? In connection with questions (2)(b), (2)(c), and (2)(d) it should be noted that the time dependence of the collector currents did depend upon the number of gauges in operation. Additional experimentation with these gauges and a quadrupole partial pressure analyzer was carried out in an attempt to assess the relative importance of the physical processes listed above. The results of this additional work, to be described in a later publication, indicate that the time dependence of the currents was in fact due to a time-dependent total pressure caused by pumping of H_2 by thermal dissociation at the hot filaments, and an associated production of other species (primarily $CO + C_2H_4$) via chemical reactions of H_2 with the material of the hot filaments. These results strongly suggest that the gauge property *sensitivity* as defined in Eq. (1), is independent of pressure and time in H_2 , as well as in N_2 and He , over the pressure range investigated in this work.

2. Sensitivity ratio determinations in H_2

Sensitivity ratios in H_2 were determined for 15 gauges. The reference gauge was the same upper chamber EXG (gauge No. 14) as used for the sensitivity ratio measurements in N_2 . The 13 cm diam conductance was used and the gas was admitted via the TMP vent port (inlet C). The magnitude of $\Delta P(H_2)$ ranged from about $0.1 \times P^\circ$ to $1000 \times P^\circ$. The data analysis was the same as that applied in the case of N_2 and He . As the ratio data exhibited no repeatable pressure dependence over the interval $3 \times 10^{-8} \text{ Pa} \leq \Delta P(H_2) \leq 3 \times 10^{-6} \text{ Pa}$, an average ratio \bar{R} was calculated for this $\Delta P(H_2)$ range. The results for all 15 gauges are shown in

Fig. 4(b), without identifying individual gauges. The abscissa for each ratio value plotted in Fig. 4(b) was determined from the absolute sensitivity value S_0 [H_2], (Table II) determined (See Sec. IV C 1) for the reference gauge at 3×10^{-5} Pa.

For pressure increments between 5×10^{-8} Pa and 1×10^{-6} Pa, these data indicate a pressure independent sensitivity ratio for each gauge pair, within an uncertainty of about $\pm 4\%$. The larger spread evident in the ratio values shown in Fig. 4(b) for $\Delta P(H_2)$ greater than about 10^{-6} Pa appeared to be the result of some systematic rather than random error in the data. For gauges No. 1, 7, 9, and 15, the data yielded sensitivity ratio values which increased with pressure between about 10^{-7} and 10^{-6} Pa and decreased for higher pressures. For the rest of the gauges, the ratios remained constant up to about 10^{-6} Pa and decreased for larger pressures.

The results shown in Fig. 4(c) were obtained by applying the ratio analysis used in Fig. 4(b) to the data set used in Fig. 4(a). In Fig. 4(c), the average ratio \bar{R} for each gauge is the arithmetic average of ratios of corresponding current changes $(I_c - I_c^\circ)_{\text{gauge}}$ and $(I_c - I_c^\circ)_{\text{ref. gauge}}$, obtained for $3 \times 10^{-8} \text{ Pa} \leq \Delta P(H_2) \leq 3 \times 10^{-6} \text{ Pa}$. It is interesting that this alternate analysis of the Fig. 4(a) data revealed very little systematic pressure dependence in the sensitivity ratios (ratios constant within $\pm 4\%$) down to $\Delta P(H_2)$ about 3×10^{-8} Pa. According to the argument given in Sec. III D, this strongly suggests that the pressure dependence seen in the absolute sensitivity data shown in Fig. 4(a) is only apparent, and in fact is due to real time dependence in the H_2 pressure (see question (2) of Sec. IV C 1). The disagreement between the ratio results shown in Fig. 4(b) and Fig. 4(c) for $\Delta P > 10^{-6}$ Pa is somewhat puzzling. They were expected to be very nearly the same, because these two figures were generated by applying the same analysis to two independently determined sets of collector current measurements. The reason for this disagreement has not yet been discovered.

The primary objective in this work was to look for pressure dependence in the gauges' sensitivities at pressures below 10^{-6} Pa. While not a proof, the fact that the ratio analysis, when applied to the absolute sensitivity results shown in Fig. 4(a), yields the comparatively pressure independent plot of Fig. 4(c) is considered to be strong evidence that:

(1) all the gauges have a pressure independent H_2 sensitivity for pressure steps $5 \times 10^{-8} \text{ Pa} \leq \Delta P(H_2) \leq 1 \times 10^{-5} \text{ Pa}$ with respect to the base pressure P° of about 5×10^{-8} Pa H_2 and that,

(2) the apparent pressure dependence seen in the absolute sensitivity results shown in Fig. 4(a) is an artifact principally due to a discrepancy between the H_2 pressure step ΔP as calculated from the operating parameters of the primary standard and the actual pressure change in the chamber.

V. CONCLUSIONS

The behavior of the Bayard-Alpert and extractor ionization gauges employed in this investigation is consistent with

a linear response in N_2 and He (i.e., constant sensitivities within an uncertainty of about $\pm 4\%$) over the pressure range 10^{-7} – 10^{-4} Pa. Because of the absence of any clear pressure dependence in the gauge-to-gauge sensitivity ratio values, as well as in the absolute sensitivity values, it is concluded that these gauges are in fact linear in their response to N_2 and He over this pressure range.

While not conclusive, the absence of any pressure dependence (within an uncertainty of about $\pm 4\%$) in the gauge-to-gauge sensitivity ratio results in H_2 is strong evidence that all the tested gauges also are linear in their response to H_2 over the pressure range 10^{-7} – 10^{-4} Pa. The apparent pressure dependence exhibited by all the gauges in their absolute H_2 sensitivity is believed to be an artifact resulting from pumping of H_2 by the gauges' hot filaments and associated production of other species such as CO and C_2H_4 .

ACKNOWLEDGMENTS

The authors thank our colleague C. R. Tilford for useful discussions of this work and critical reading of the manuscript, and the United States Department of Energy for financial support.

^{a)} Previous publications under the name Sharrill D. Wood.

^{b)} Formerly known as the National Bureau of Standards (NBS).

¹ R. T. Bayard and D. Alpert, *Rev. Sci. Instrum.* **21**, 571 (1950).

² P. A. Readhead, *J. Vac. Sci. Technol.* **7**, 182 (1970).

³ A. R. Filippelli, *J. Vac. Sci. Technol. A* **5**, 3234 (1987).

⁴ H. C. Hseuh and C. Lanni, *J. Vac. Sci. Technol. A* **5**, 3244 (1987).

⁵ K. E. McCulloh and C. R. Tilford, *J. Vac. Sci. Technol.* **18**, 994 (1981).

⁶ C. R. Tilford, *J. Vac. Sci. Technol. A* **3**, 546 (1985).

⁷ G. Grosse and G. Messer, *Vak. Tech.* **30**, 226 (1981).

⁸ B. Angerth, *Vacuum* **22**, 7 (1972).

⁹ W. D. Davis, *J. Vac. Sci. Technol.* **5**, 23 (1968).

¹⁰ J. R. Roehrig and J. C. Simons, Jr., in *Transactions of the American Vacuum Society Symposium*, 1961 (Pergamon, New York, 1962), Vol. 8, p. 511.

¹¹ D. Alpert and R. S. Buritz, *J. Appl. Phys.* **25**, 202 (1954).

¹² D. Alpert, in *Handbuch der Physik* (Springer-Verlag, Wurzburg, 1958), Vol. 12, p. 617.

¹³ S. Dittmann, High Vacuum Standard and Its Use, National Institute of Standards and Technology (NIST) Special Publication SP 250-34 (1989).

¹⁴ C. R. Tilford, S. Dittmann, and K. E. McCulloh, *J. Vac. Sci. Technol. A* **6**, 2853 (1988).

¹⁵ K. E. McCulloh, C. R. Tilford, C. D. Ehrlich, and F. G. Long, *J. Vac. Sci. Technol. A* **5**, 376 (1987).

¹⁶ J. K. Fremerey, *Vacuum* **32**, 685 (1982).

¹⁷ J. K. Fremerey, *J. Vac. Sci. Technol. A* **3**, 1715 (1985).

¹⁸ J. G. Werner and J. H. Leck, *J. Sci. Instrum.* **2**, 861 (1969).

¹⁹ G. Messer, *Phys. Bl* **33**, 343 (1977); in *Proceedings of the 7th International Vacuum Congress and the 3rd International Conference on Solid Surfaces*, 1977 (Berger and Söhne, Horn, Austria, 1977), Vol. 1, p. 153.

²⁰ T. W. Hickmott, *J. Appl. Phys.* **31**, 128 (1960).

²¹ T. W. Hickmott, *J. Chem. Phys.* **32**, 810 (1960).

²² J. N. Smith, Jr. and W. L. Fite, *J. Chem. Phys.* **37**, 898 (1962).

²³ G. E. Moore and F. C. Unterwald, *J. Chem. Phys.* **40**, 2639 (1964).

²⁴ T. W. Hickmott, *J. Vac. Sci. Technol.* **2**, 257 (1965).

²⁵ S. J. B. Corrigan, *J. Chem. Phys.* **43**, 4381 (1965).

²⁶ S. Chung and C. C. Lin, *Phys. Rev. A* **17**, 1874 (1978).